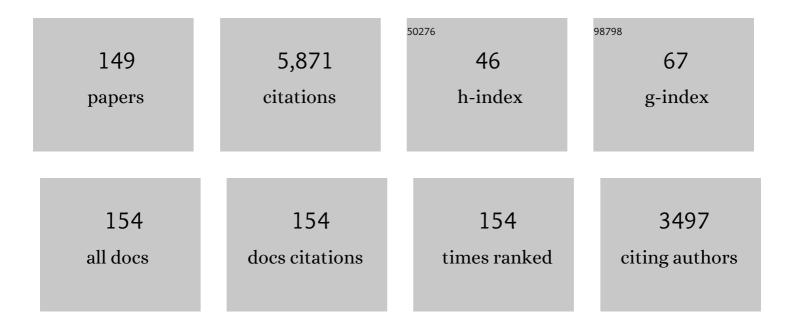
Dave Phillips

List of Publications by Year in descending order

Source: https://exaly.com/author-pdf/1079922/publications.pdf Version: 2024-02-01



DAVE DHILLIDS

#	Article	IF	CITATIONS
1	High abundances of noble gas and chlorine delivered to the mantle by serpentinite subduction. Nature Geoscience, 2011, 4, 807-812.	12.9	201
2	Subduction zone fluxes of halogens and noble gases in seafloor and forearc serpentinites. Earth and Planetary Science Letters, 2013, 365, 86-96.	4.4	137
3	Ultra-high precision 40Ar/39Ar ages for Fish Canyon Tuff and Alder Creek Rhyolite sanidine: New dating standards required?. Geochimica Et Cosmochimica Acta, 2013, 121, 229-239.	3.9	134
4	The Fish Canyon Tuff: A new look at an old low-temperature thermochronology standard. Earth and Planetary Science Letters, 2015, 424, 95-108.	4.4	133
5	Subduction-related diamonds? — The evidence for a mantle-derived origin from coupled δ13C–δ15N determinations. Chemical Geology, 1998, 147, 147-159.	3.3	116
6	Constraints on kimberlite ascent mechanisms revealed by phlogopite compositions in kimberlites and mantle xenoliths. Lithos, 2016, 240-243, 189-201.	1.4	111
7	Mesozoic Orogenic Gold Mineralization in the Jiaodong Peninsula, China: A Focused Event at 120 ± 2 Ma During Cooling of Pregold Granite Intrusions. Economic Geology, 2020, 115, 415-441.	3.8	110
8	Interpreting and reporting 40Ar/39Ar geochronologic data. Bulletin of the Geological Society of America, 2021, 133, 461-487.	3.3	102
9	Argon isotopic zoning in mantle phlogopite. Geology, 1988, 16, 542.	4.4	97
10	Provenance ages of the Neoproterozoic Katanga Supergroup (Central African Copperbelt), with implications for basin evolution. Journal of African Earth Sciences, 2005, 42, 41-60.	2.0	97
11	Data reporting norms for 40Ar/39Ar geochronology. Quaternary Geochronology, 2009, 4, 346-352.	1.4	97
12	The Kalkarindji continental flood basalt province: A new Cambrian large igneous province in Australia with possible links to faunal extinctions. Geology, 2006, 34, 461.	4.4	96
13	Nature of alkali-carbonate fluids in the sub-continental lithospheric mantle. Geology, 2012, 40, 967-970.	4.4	88
14	Petrogenesis of Mantle Polymict Breccias: Insights into Mantle Processes Coeval with Kimberlite Magmatism. Journal of Petrology, 2014, 55, 831-858.	2.8	86
15	Halogen systematics (Cl, Br, I) in Mid-Ocean Ridge Basalts: A Macquarie Island case study. Geochimica Et Cosmochimica Acta, 2012, 81, 82-93.	3.9	83
16	Evolution of a reworked orogenic zone: The boundary between the delamerian and lachlan fold belts, southeastern Australia *. Australian Journal of Earth Sciences, 2005, 52, 921-940.	1.0	81
17	Stable isotope (C, O, S) compositions of volatile-rich minerals in kimberlites: A review. Chemical Geology, 2014, 374-375, 61-83.	3.3	81
18	New insights into the genesis of Indian kimberlites from the Dharwar Craton via in situ Sr isotope analysis of groundmass perovskite. Geology, 2007, 35, 1011.	4.4	78

#	Article	IF	CITATIONS
19	African kimberlites revisited: In situ Sr-isotope analysis of groundmass perovskite. Lithos, 2009, 112, 311-317.	1.4	78
20	Did diamond-bearing orangeites originate from MARID-veined peridotites in the lithospheric mantle?. Nature Communications, 2015, 6, 6837.	12.8	78
21	The final stages of kimberlite petrogenesis: Petrography, mineral chemistry, melt inclusions and Sr-C-O isotope geochemistry of the Bultfontein kimberlite (Kimberley, South Africa). Chemical Geology, 2017, 455, 342-356.	3.3	78
22	Oxide, sulphide and carbonate minerals in a mantle polymict breccia: Metasomatism by proto-kimberlite magmas, and relationship to the kimberlite megacrystic suite. Chemical Geology, 2013, 353, 4-18.	3.3	77
23	Mineral chemistry and thermobarometry of inclusions from De Beers Pool diamonds, Kimberley, South Africa. Lithos, 2004, 77, 155-179.	1.4	75
24	Kimberlite genesis from a common carbonate-rich primary melt modified by lithospheric mantle assimilation. Science Advances, 2020, 6, eaaz0424.	10.3	72
25	Chlorine from the mantle: Magmatic halides in the Udachnaya-East kimberlite, Siberia. Earth and Planetary Science Letters, 2009, 285, 96-104.	4.4	70
26	High-precision dating of the Kalkarindji large igneous province, Australia, and synchrony with the Early–Middle Cambrian (Stage 4–5) extinction. Geology, 2014, 42, 543-546.	4.4	70
27	Petrology and Nd–Hf Isotope Geochemistry of the Neoproterozoic Amon Kimberlite Sills, Baffin Island (Canada): Evidence for Deep Mantle Magmatic Activity Linked to Supercontinent Cycles. Journal of Petrology, 2014, 55, 2003-2042.	2.8	69
28	Astronomical calibration of 40Ar/39Ar reference minerals using high-precision, multi-collector (ARGUSVI) mass spectrometry. Geochimica Et Cosmochimica Acta, 2017, 196, 351-369.	3.9	67
29	Monazite U–Pb dating and 40Ar–39Ar thermochronology of metamorphic events in the Central African Copperbelt during the Pan-African Lufilian Orogeny. Journal of African Earth Sciences, 2005, 42, 183-199.	2.0	66
30	Thermochronological (⁴⁰ Ar/ ³⁹ Ar) evidence of Early Palaeozoic basin inversion within the southern Prince Charles Mountains, East Antarctica: implications for East Gondwana. Journal of the Geological Society, 2007, 164, 771-784.	2.1	66
31	Mid-crustal fluid mixing in a Proterozoic Fe oxide–Cu–Au deposit, Ernest Henry, Australia: Evidence from Ar, Kr, Xe, Cl, Br, and I. Earth and Planetary Science Letters, 2007, 256, 328-343.	4.4	65
32	Kimberlites reveal 2.5-billion-year evolution of a deep, isolated mantle reservoir. Nature, 2019, 573, 578-581.	27.8	64
33	The halogen (F, Cl, Br, I) and H2O systematics of Samoan lavas: Assimilated-seawater, EM2 and high-3He/4He components. Earth and Planetary Science Letters, 2015, 410, 197-209.	4.4	62
34	Laser microprobe measurement of chlorine and argon zonation in biotite. Chemical Geology, 1991, 90, 145-168.	3.3	61
35	The tectonostratigraphy, granitoid geochronology and geological evolution of the Precambrian of southern Ethiopia. Journal of African Earth Sciences, 2002, 34, 57-84.	2.0	61
36	Timing and modes of granite magmatism in the core of the Alboran Domain, Rif chain, northern Morocco: Implications for the Alpine evolution of the western Mediterranean. Tectonics, 2010, 29, n/a-n/a.	2.8	59

#	Article	IF	CITATIONS
37	A new approach to reconstructing the composition and evolution of kimberlite melts: A case study of the archetypal Bultfontein kimberlite (Kimberley, South Africa). Lithos, 2018, 304-307, 1-15.	1.4	58
38	Mesozoic cooling across the Yidun Arc, central-eastern Tibetan Plateau: A reconnaissance 40Ar/39Ar study. Tectonophysics, 2005, 398, 45-66.	2.2	57
39	In-situ assimilation of mantle minerals by kimberlitic magmas — Direct evidence from a garnet wehrlite xenolith entrained in the Bultfontein kimberlite (Kimberley, South Africa). Lithos, 2016, 256-257, 182-196.	1.4	57
40	Identifying the asthenospheric component of kimberlite magmas from the Dharwar Craton, India. Lithos, 2009, 112, 296-310.	1.4	56
41	Porphyry and Epithermal Deposits and 40Ar/39Ar Geochronology of the Baguio District, Philippines. Economic Geology, 2011, 106, 1335-1363.	3.8	56
42	40Ar/39Ar laser-probe dating of diamond inclusions from the Premier kimberlite. Nature, 1989, 340, 460-462.	27.8	55
43	40Ar/39Ar thermochronology of the Kampa Dome, southern Tibet: Implications for tectonic evolution of the North Himalayan gneiss domes. Tectonophysics, 2006, 421, 269-297.	2.2	53
44	Thermochronology of the Yidun Arc, central eastern Tibetan Plateau: constraints from 40Ar/39Ar K-feldspar and apatite fission track data. Journal of Asian Earth Sciences, 2005, 25, 915-935.	2.3	52
45	New geochemical constraints on the origins of MARID and PIC rocks: Implications for mantle metasomatism and mantle-derived potassic magmatism. Lithos, 2018, 318-319, 478-493.	1.4	50
46	40Ar/39Ar and K–Ar age constraints on the timing of regional deformation, south coast of New South Wales, Lachlan Fold Belt: Problems and implications. Australian Journal of Earth Sciences, 2001, 48, 395-408.	1.0	48
47	Timing of gold mineralisation in the western Lachlan Orogen, SE Australia: A critical overview. Australian Journal of Earth Sciences, 2012, 59, 495-525.	1.0	47
48	Late Cretaceous–earliest Paleogene deformation in the Longmen Shan foldâ€andâ€thrust belt, eastern Tibetan Plateau margin: Pre enozoic thickened crust?. Tectonics, 2016, 35, 2293-2312.	2.8	46
49	Early Palaeozoic intracratonic shears and post-tectonic cooling in the Rauer Group, Prydz Bay, East Antarctica constrained by40Ar/39Ar thermochronology. Antarctic Science, 2007, 19, 339-353.	0.9	45
50	The Cambrian Kalkarindji Large Igneous Province: Extent and characteristics based on new 40Ar/39Ar and geochemical data. Lithos, 2009, 110, 294-304.	1.4	44
51	Sulfur isotope composition of metasomatised mantle xenoliths from the Bultfontein kimberlite (Kimberley, South Africa): Contribution from subducted sediments and the effect of sulfide alteration on S isotope systematics. Earth and Planetary Science Letters, 2016, 445, 114-124.	4.4	43
52	Petrographic and melt-inclusion constraints on the petrogenesis of a magmaclast from the Venetia kimberlite cluster, South Africa. Chemical Geology, 2017, 455, 331-341.	3.3	43
53	Origin of complex zoning in olivine from diverse, diamondiferous kimberlites and tectonic settings: Ekati (Canada), Alto Paranaiba (Brazil) and Kaalvallei (South Africa). Mineralogy and Petrology, 2018, 112, 539-554.	1.1	43
54	Progressive metasomatism of the mantle by kimberlite melts: Sr–Nd–Hf–Pb isotope compositions of MARID and PIC minerals. Earth and Planetary Science Letters, 2019, 509, 15-26.	4.4	43

#	Article	IF	CITATIONS
55	Noble gas and halogen constraints on regionally extensive mid-crustal Na–Ca metasomatism, the Proterozoic Eastern Mount Isa Block, Australia. Precambrian Research, 2008, 163, 131-150.	2.7	42
56	Halogens and noble gases in sedimentary formation waters and Zn–Pb deposits: A case study from the Lennard Shelf, Australia. Applied Geochemistry, 2011, 26, 2089-2100.	3.0	41
57	LIMA U–Pb ages link lithospheric mantle metasomatism to Karoo magmatism beneath the Kimberley region, South Africa. Earth and Planetary Science Letters, 2014, 401, 132-147.	4.4	41
58	Part I. Decrepitation and degassing behaviour of quartz up to 1560°C: Analysis of noble gases and halogens in complex fluid inclusion assemblages. Geochimica Et Cosmochimica Acta, 2006, 70, 2540-2561.	3.9	40
59	New 40Ar/39Ar ages for selected young (<1ÂMa) basalt flows of the Newer Volcanic Province, southeastern Australia. Quaternary Geochronology, 2011, 6, 356-368.	1.4	40
60	New constraints on fluid sources in orogenic gold deposits, Victoria, Australia. Contributions To Mineralogy and Petrology, 2012, 163, 427-447.	3.1	40
61	Noble gas and halogen constraints on mineralizing fluids of metamorphic versus surficial origin: Mt Isa, Australia. Chemical Geology, 2006, 235, 325-351.	3.3	39
62	Petrogenesis of a Hybrid Cluster of Evolved Kimberlites and Ultramafic Lamprophyres in the Kuusamo Area, Finland. Journal of Petrology, 2019, 60, 2025-2050.	2.8	37
63	The noble gas systematics of late-orogenic H2O–CO2 fluids, Mt Isa, Australia. Geochimica Et Cosmochimica Acta, 2011, 75, 1428-1450.	3.9	35
64	High precision multi-collector 40Ar/39Ar dating of young basalts: Mount Rouse volcano (SE) Tj ETQq0 0 0 rgBT /	Overlock 1 1.4	10 Tf 50 382 T
65	Argon isotope and halogen chemistry of phlogopite from South African kimberlites: a combined step-heating, laser probe, electron microprobe and TEM study. Chemical Geology: Isotope Geoscience Section, 1991, 87, 71-98.	0.6	34
66	Redetermination of the 21Ne relative abundance of the atmosphere, using a high resolution, multi-collector noble gas mass spectrometer (HELIX-MC Plus). International Journal of Mass Spectrometry, 2015, 387, 1-7.	1.5	34
67	Kimberlite-related metasomatism recorded in MARID and PIC mantle xenoliths. Mineralogy and Petrology, 2018, 112, 71-84.	1.1	34
68	Pressure-temperature-deformation-time (P-T-d-t) exhumation history of the Voltri Massif HP complex, Ligurian Alps, Italy. Tectonics, 2010, 29, n/a-n/a.	2.8	33
69	Geochronological Constraints on the Tropicana Gold Deposit and Albany-Fraser Orogen, Western Australia. Economic Geology, 2015, 110, 355-386.	3.8	33
70	Dating Kimberlites: Methods and Emplacement Patterns Through Time. Elements, 2019, 15, 399-404.	0.5	33
71	40Ar/39Ar dating of mica-bearing pyrite from thermally overprinted Archean gold deposits. Geology, 2006, 34, 397.	4.4	32
72	Tracking continental-scale modification of the Earth's mantle using zircon megacrysts. Geochemical Perspectives Letters, 0, , 1-6.	5.0	32

5

#	Article	IF	CITATIONS
73	Unusual noble gas compositions in polycrystalline diamonds: preliminary results from the Jwaneng kimberlite, Botswana. Chemical Geology, 2004, 203, 347-358.	3.3	31
74	The Origin and Evolution of Mineralizing Fluids in a Sediment-Hosted Orogenic-Gold Deposit, Ballarat East, Southeastern Australia. Economic Geology, 2011, 106, 653-666.	3.8	31
75	Mantle oddities: A sulphate fluid preserved in a MARID xenolith from the Bultfontein kimberlite (Kimberley, South Africa). Earth and Planetary Science Letters, 2013, 376, 74-86.	4.4	31
76	New constraints on the release of noble gases during in vacuo crushing and application to scapolite Br–Cl–I and 40Ar/39Ar age determinations. Geochimica Et Cosmochimica Acta, 2009, 73, 5673-5692.	3.9	30
77	Isotopic ages of Lentiira - Kuhmo - Kostomuksha olivine lamproite - Group II kimberlites. Bulletin of the Geological Society of Finland, 2007, 79, 203-215.	0.8	30
78	Controls on Skarn Mineralization and Alteration at the Cadia Deposits, New South Wales, Australia. Economic Geology, 2004, 99, 761-788.	3.8	29
79	Compressional reworking of the East African Orogen in the Uluguru Mountains of eastern Tanzania at <i>c.</i> 550 Ma: implications for the final assembly of Gondwana. Terra Nova, 2008, 20, 59-67.	2.1	29
80	Stratigraphy, geochronology and evolution of the Mt. Melbourne volcanic field (North Victoria Land,) Tj ETQqO 0	0 rgBT /O	verlgck 10 Tf
81	Crystallisation sequence and magma evolution of the De Beers dyke (Kimberley, South Africa). Mineralogy and Petrology, 2018, 112, 503-518.	1.1	29
82	The role of lithospheric heterogeneity on the composition of kimberlite magmas from a single field: The case of Kaavi-Kuopio, Finland. Lithos, 2020, 354-355, 105333.	1.4	29
83	Highâ€pressure metamorphism in the southern New England Orogen: Implications for longâ€lived accretionary orogenesis in eastern Australia. Tectonics, 2015, 34, 1979-2010.	2.8	28
84	Kimberlite Metasomatism of the Lithosphere and the Evolution of Olivine in Carbonate-rich Melts — Evidence from the Kimberley Kimberlites (South Africa). Journal of Petrology, 2020, 61, .	2.8	28
85	Structure, detrital zircon U – Pb ages and40Ar/39Ar geochronology of the Early Palaeozoic Girilambone Group, central New South Wales: subduction, contraction and extension associated with the Benambran Orogeny. Australian Journal of Earth Sciences, 2005, 52, 137-159.	1.0	27
86	Nickel-rich metasomatism of the lithospheric mantle by pre-kimberlitic alkali-S–Cl-rich C–O–H fluids. Contributions To Mineralogy and Petrology, 2013, 165, 155-171.	3.1	26
87	Re–Os and 40Ar/39Ar isotope measurements of inclusions in alluvial diamonds from the Ural Mountains: Constraints on diamond genesis and eruption ages. Lithos, 2009, 112, 714-723.	1.4	25
88	Ancient metasomatism recorded by ultra-depleted garnet inclusions in diamonds from DeBeers Pool, South Africa. Lithos, 2009, 112, 736-746.	1.4	25

89	New constraints on regional brecciation in the Wernecke Mountains, Canada, from He, Ne, Ar, Kr, Xe, Cl, Br and I in fluid inclusions. Chemical Geology, 2008, 255, 33-46.	3.3	24
90	Part II. Evaluation of 40Ar–39Ar quartz ages: Implications for fluid inclusion retentivity and determination of initial 40Ar/36Ar values in Proterozoic samples. Geochimica Et Cosmochimica Acta,	3.9	22

90determination of initial 40Ar/36Ar values in Proterozoic samples. Geochimica Et Cosmochimica Acta,
2006, 70, 2562-2576.3.9

#	Article	IF	CITATIONS
91	⁴⁰ Ar/ ³⁹ Ar geochronology reveals rapid change from plumeâ€assisted to stressâ€dependent volcanism in the Newer Volcanic Province, SE Australia. Geochemistry, Geophysics, Geosystems, 2017, 18, 1065-1089.	2.5	22
92	Application of ³⁶ / ⁴⁰ Ar Versus ³⁹ Ar/ ⁴⁰ Ar Correlation diagrams to the ⁴⁰ Ar/ ³⁹ Ar spectra of phlogopites from Southern African kimberlites. Geophysical Research Letters, 1986, 13, 689-692.	4.0	21
93	The nature of magmatism at Palinpinon geothermal field, Negros Island, Philippines: implications for geothermal activity and regional tectonics. Journal of Volcanology and Geothermal Research, 2004, 129, 321-342.	2.1	20
94	40Ar/39Ar analyses of clinopyroxene inclusions in African diamonds: implications for source ages of detrital diamonds. Geochimica Et Cosmochimica Acta, 2004, 68, 151-165.	3.9	20
95	Magnetic and chemical stratigraphy for the Werribee Plains basaltic lava flow-field, Newer Volcanics Province, southeast Australia: implications for eruption frequency. Australian Journal of Earth Sciences, 2005, 52, 41-57.	1.0	20
96	The Palaeozoic tectono-metallogenic evolution of the northern Tasman Fold Belt System, Australia: Interplay of subduction rollback and accretion. Ore Geology Reviews, 2007, 30, 277-296.	2.7	20
97	Structure of the Early Palaeozoic Cape River Metamorphics, Tasmanides of north Queensland: evaluation of the roles of convergent and extensional tectonics. Australian Journal of Earth Sciences, 2005, 52, 261-277.	1.0	18
98	An Overview of Cape Fold Belt Geochronology: Implications for Sediment Provenance and the Timing of Orogenesis. Regional Geology Reviews, 2016, , 45-55.	1.2	18
99	Siliciclastic record of rapid denudation in response to convergent-margin orogenesis, Ross Orogen, Antarctica. , 2004, , .		18
100	Geochronology of Diamonds. Reviews in Mineralogy and Geochemistry, 2022, 88, 567-636.	4.8	18
101	Structural, metamorphic, and geochronological constraints on alternating compression and extension in the Early Paleozoic Gondwanan Pacific margin, northeastern Australia. Tectonics, 2007, 26, n/a-n/a.	2.8	17
102	Evolution of Ataúro Island: Temporal constraints on subduction processes beneath the Wetar zone, Banda Arc. Journal of Asian Earth Sciences, 2011, 41, 477-493.	2.3	17
103	Apatite compositions and groundmass mineralogy record divergent melt/fluid evolution trajectories in coherent kimberlites caused by differing emplacement mechanisms. Contributions To Mineralogy and Petrology, 2020, 175, 1.	3.1	17
104	The spatial and temporal evolution of primitive melt compositions within the Lac de Gras kimberlite field, Canada: Source evolution vs lithospheric mantle assimilation. Lithos, 2021, 392-393, 106142.	1.4	17
105	A comparison of geochronological methods commonly applied to kimberlites and related rocks: Three case studies from Finland. Chemical Geology, 2020, 558, 119899.	3.3	16
106	Provenance studies from 40Ar/39Ar dating of mineral inclusions in diamonds: Methodological tests on the Orapa kimberlite, Botswana. Earth and Planetary Science Letters, 2008, 274, 169-178.	4.4	15
107	Lake Boga Granite, northwestern Victoria: mineralogy, geochemistry and geochronology. Australian Journal of Earth Sciences, 2008, 55, 281-299.	1.0	15
108	Detrital zircon U–Pb and ⁴⁰ Ar/ ³⁹ Ar hornblende ages from the Aileu Complex, Timor-Leste: provenance and metamorphic cooling history. Journal of the Geological Society, 2014, 171, 299-309.	2.1	15

#	Article	IF	CITATIONS
109	CH4-N2 in the Maldon gold deposit, central Victoria, Australia. Ore Geology Reviews, 2014, 58, 225-237.	2.7	15
110	An evidence-based approach to accurate interpretation of 40Ar/39Ar ages from basaltic rocks. Earth and Planetary Science Letters, 2018, 498, 65-76.	4.4	15
111	Early human occupation of southeastern Australia: New insights from 40Ar/39Ar dating of young volcanoes. Geology, 2020, 48, 390-394.	4.4	15
112	The Timing of Mineralization in the Archean North Pilbara Terrain, WesternAustralia. Economic Geology, 2002, 97, 733-755.	3.8	14
113	Perturbation of the deep-Earth carbon cycle in response to the Cambrian Explosion. Science Advances, 2022, 8, eabj1325.	10.3	14
114	Timing of Alpine Orogeny and Postorogenic Extension in the Alboran Domain, Inner Rif Chain, Morocco. Tectonics, 2021, 40, e2021TC006707.	2.8	13
115	Strontium Isotope Analysis of Kimberlitic Groundmass Perovskite via LA-MC-ICP-MS. Geostandards and Geoanalytical Research, 2007, 31, 071117031212001-???.	1.9	12
116	Comment on "New Ar–Ar ages of southern Indian kimberlites and a lamproite and their geochemical evolution―by Osborne et al. [Precambrian Res. 189 (2011) 91–103]. Precambrian Research, 2012, 208-211, 49-52.	2.7	12
117	Stratigraphy and ⁴⁰ Ar/ ³⁹ Ar geochronology of the Santa Rosa basin, Baja California: Dynamic evolution of a constrictional rift basin during oblique extension in the Gulf of California. Basin Research, 2013, 25, 388-418.	2.7	12
118	Provenance of Cape Supergroup sediments and timing of Cape Fold Belt orogenesis: Constraints from high-precision 40Ar/39Ar dating of muscovite. Gondwana Research, 2019, 70, 201-221.	6.0	12
119	Thermotectonic evolution of the western margin of the Yilgarn craton, Western Australia: New insights from 40 Ar/ 39 Ar analysis of muscovite and biotite. Precambrian Research, 2015, 270, 139-154.	2.7	11
120	Titanates of the lindsleyite–mathiasite (LIMA) group reveal isotope disequilibrium associated with metasomatism in the mantle beneath Kimberley (South Africa). Earth and Planetary Science Letters, 2018, 482, 253-264.	4.4	11
121	Noble gas geochemistry of fluid inclusions in South African diamonds: implications for the origin of diamond-forming fluids. Mineralogy and Petrology, 2018, 112, 181-195.	1.1	11
122	Controls on the explosive emplacement of diamondiferous kimberlites: New insights from hypabyssal and pyroclastic units in the Diavik mine, Canada. Lithos, 2020, 360-361, 105410.	1.4	11
123	The geochemistry, petrogenesis and age of an unusual alkaline intrusion in the western Pilbara craton, Western Australia. Lithos, 2009, 112, 419-428.	1.4	10
124	Diamond provenance studies from 40Ar/39Ar dating of clinopyroxene inclusions: An example from the west coast of Namibia. Lithos, 2009, 112, 793-805.	1.4	10
125	⁴⁰ Ar/ ³⁹ Ar and K–Ar ages: early Paleozoic metamorphism and deformation in the Narooma accretionary complex, NSW. Australian Journal of Earth Sciences, 2011, 58, 21-32.	1.0	10
126	Provenance history of detrital diamond deposits, West Coast of Namaqualand, South Africa. Mineralogy and Petrology, 2018, 112, 259-273.	1.1	10

#	Article	IF	CITATIONS
127	Revised astronomically calibrated 40Ar/39Ar ages for the Fish Canyon Tuff sanidine – Closing the interlaboratory gap. Chemical Geology, 2022, 597, 120815.	3.3	10
128	He, Ne and Ar in peridotitic and eclogitic paragenesis diamonds from the Jwaneng kimberlite, Botswana—Implications for mantle evolution and diamond formation ages. Earth and Planetary Science Letters, 2011, 301, 43-51.	4.4	9
129	40Ar/39Ar ages of alkali feldspar xenocrysts constrain the timing of intraplate basaltic volcanism. Quaternary Geochronology, 2018, 47, 14-28.	1.4	9
130	Petrogenesis of coeval lamproites and kimberlites from the Wajrakarur field, Southern India: New insights from olivine compositions. Lithos, 2021, 406-407, 106524.	1.4	8
131	AusGeochem: An Open Platform for Geochemical Data Preservation, Dissemination and Synthesis. Geostandards and Geoanalytical Research, 2022, 46, 245-259.	3.1	8
132	Noble gas and carbon isotope ratios in Argyle diamonds, Western Australia: Evidence for a deeply subducted volatile component. Australian Journal of Earth Sciences, 2012, 59, 1135-1142.	1.0	7
133	Episodic gold mineralisation correlated with discrete structural events at Ballarat East, southeast Australia. Ore Geology Reviews, 2017, 91, 541-558.	2.7	7
134	Quaternary volcanic evolution in the continental back-arc of southern Mendoza, Argentina. Journal of South American Earth Sciences, 2018, 84, 88-103.	1.4	7
135	Geochronological, morphometric and geochemical constraints on the Pampas Onduladas long basaltic flow (Payún Matrú Volcanic Field, Mendoza, Argentina). Journal of Volcanology and Geothermal Research, 2014, 289, 114-129.	2.1	6
136	40Ar/39Ar dating of alkali feldspar megacrysts from selected young volcanoes of the Newer Volcanic Province, Victoria. Proceedings of the Royal Society of Victoria, 2013, 125, 59.	0.4	6
137	Discussion of â€`the Paleozoic metamorphic history of the Central Orogenic Belt of China from 40Ar/39Ar geochronology of eclogite garnet fluid inclusions by Qiu Hua-Ning and Wijbrans J.R.'. Earth and Planetary Science Letters, 2009, 279, 392-394.	4.4	5
138	A new ⁴⁰ Ar/ ³⁹ Ar eruption age for the Mount Widderin volcano, Newer Volcanic Province, Australia, with implications for eruption frequency in the region. Australian Journal of Earth Sciences, 2016, 63, 175-186.	1.0	5
139	Basalt lava flows of the intraplate Newer Volcanic Province in south-east Australia (Melbourne) Tj ETQq1 1 0.784 Geothermal Research, 2020, 389, 106730.	314 rgBT / 2.1	Overlock 10 5
140	Structural evolution and tectonic context of the Mfongosi Group, Natal thrust front, Tugela terrane, South Africa. Journal of African Earth Sciences, 2005, 43, 415-432.	2.0	4
141	Geodynamic and Isotopic Constraints on the Genesis of Kimberlites, Lamproites and Related Magmas From the Finnish Segment of the Karelian Craton. Geochemistry, Geophysics, Geosystems, 2022, 23, .	2.5	4
142	Controls on the Emplacement Style of Coherent Kimberlites in the Lac de Gras Field, Canada. Journal of Petrology, 2022, 63, .	2.8	3
143	Petrography, Sr-isotope geochemistry and geochronology of the Nxau Nxau kimberlites, north-west Botswana. Mineralogy and Petrology, 2018, 112, 625-638.	1.1	2
144	40Ar/39Ar geochronology of the Pongkor low sulfidation epithermal gold mineralisation, West Java, Indonesia. Ore Geology Reviews, 2020, 119, 103341.	2.7	2

#	Article	IF	CITATIONS
145	⁴⁰ Ar/ ³⁹ Ar Geochronology of Volcanic and Intrusive Rocks in the Papandayan Metallic Prospect Area, West Java, Indonesia. Resource Geology, 2017, 67, 53-71.	0.8	1
146	Reply to Murray-Wallace, C.V. Comment on Matchan and Phillips, 2011. New 40Ar/39Ar ages for selected young (<1ÂMa) basalt flows of the Newer Volcanic Province, southeastern Australia. Quaternary Geochronology, 2011, 6, 600.	1.4	0
147	Production of 21Ne in depth-profiled olivine from a 54 Ma basalt sequence, Eastern Highlands (37° S), Australia. Geochimica Et Cosmochimica Acta, 2018, 220, 276-290.	3.9	0
148	Major element data, 40Ar/39Ar step-heating and step-crushing data for anorthoclase megacrysts from the Newer Volcanic Province, south-eastern Australia. Data in Brief, 2018, 19, 1847-1851.	1.0	0
149	Early Palaeozoic cooling of the southern Prince Charles Mountains, East Antarctica: Synchronous cooling of three stratigraphic levels. ASEG Extended Abstracts, 2006, 2006, 1-2.	0.1	0